

Article

Mathematical Models of Androgen Resistance in Prostate Cancer Patients under Intermittent Androgen Suppression Therapy

Javier Baez and Yang Kuang *

School of Mathematical and Statistical Sciences, Arizona State University, Tempe, AZ 85287, USA;
jbaez2@asu.edu

* Correspondence: kuang@asu.edu; Tel.: +1-480-965-6915

Academic Editor: Serafim Kalliadasis

Received: 15 August 2016; Accepted: 5 November 2016; Published: 16 November 2016

Abstract: Predicting the timing of a castrate resistant prostate cancer is critical to lowering medical costs and improving the quality of life of advanced prostate cancer patients. We formulate, compare and analyze two mathematical models that aim to forecast future levels of prostate-specific antigen (PSA). We accomplish these tasks by employing clinical data of locally advanced prostate cancer patients undergoing androgen deprivation therapy (ADT). While these models are simplifications of a previously published model, they fit data with similar accuracy and improve forecasting results. Both models describe the progression of androgen resistance. Although Model 1 is simpler than the more realistic Model 2, it can fit clinical data to a greater precision. However, we found that Model 2 can forecast future PSA levels more accurately. These findings suggest that including more realistic mechanisms of androgen dynamics in a two population model may help androgen resistance timing prediction.

Keywords: mathematical modeling; prostate cancer; androgen deprivation therapy; data fitting

1. Introduction

Ever since the discovery of androgen dependency of prostate cells, androgen deprivation therapy (ADT) has played a vital role in the treatment of metastatic and locally advanced prostate cancer [1–3]. However, controversy remains regarding its best application. Although this treatment will regress tumors in over 90% of patients [4], after prolonged androgen depletion, patients will eventually develop castration-resistant prostate cancer (CRPC) [5]. The development of CRPC can take from a few months to more than ten years [3,6], after which there is a very limited number of effective treatments and patients suffer high mortality [7]. ADT is expensive and its side effects include sexual dysfunction, hot flashes, and fatigue [8]. Based on some preclinical studies, intermittent androgen suppression (IAS) is suggested as a sensible alternative to ADT [9]. During off-treatment periods, patients enjoy a “vacation” from the severe side effects of ADT [8], and studies have suggested that IAS may not negatively affect the time to resistance progression or survival in comparison to ADT [10]. Consequently, IAS is selected by some patients to improve the quality of life and also hopefully to delay the progression to CRPC [4].

Many mathematical models have studied the dynamics of prostate cancer during ADT or IAS [11–18]. A detailed review of some of these models are presented in the recent book of Kuang et al. [19]. Ideta et al. are pioneers of mathematically modeling and analyzing the dynamics of IAS [12]. They formulated a system of ordinary differential equations to study the mechanics of ADT and IAS. They considered castrate-resistant (CR) and castrate-sensitive (CS) cell populations as well as androgen levels. Their model included mutations from CS to CR cells, and their focus was on

comparing continuous and intermittent therapy and the development of resistance. Hirata et al. [14] introduced a piece-wise linear model of three cancer cell populations. Their model included CS cells, CR cells that may mutate into CS cells, and CR cells that will not mutate. Several investigators using Hirata et al.'s model [14] have studied estimation of parameters [20,21], optimal switching times and control in IAS [20,22,23], and forecasting CRPC progression [24,25].

Built on the works of Ideta et al. [12] and Jackson [26], Portz, Kuang, and Nagy (PKN) [13] developed a novel mathematical model to study the dynamics of IAS by using the cell quota model [27] from mathematical ecology, which relates growth rate to an intracellular nutrient, to modeling the growth of both the CS and CR cell populations. The cell quota in [13] is defined as the intracellular androgen concentrations for each cell population. This model is carefully fitted with clinical prostate-specific antigen (PSA) data, where androgen data was used to model the cell quota and other growth parameters. Everett et al. [28] compared the models of Hirata et al. [14] and PKN [13] regarding their accuracy of fitting clinical data and predicting future PSA levels. They concluded that while a biologically-based model is important to reveal the underlying processes and my present more robust and better predictions, a simpler model such as that of Hirata et al. might also be practical for fitting clinical data and predicting future PSA outcomes of individual patients.

In this paper, we present a simplified model to the final model in PKN [13]. Several key terms in our model will be mechanistically formulated. This model is concise and amenable to systematical mathematical analysis of its dynamics. For simplicity, we shall use serum androgen concentration to approximate intracellular androgen. This is reasonable since androgen passively and quickly diffuses through the prostate membrane via concentration gradient [29]. This approach is practical for a typical clinical setting, where the data collected can be applied directly to the model. Most importantly, our model can fit PSA and androgen values simultaneously, which enables us to be more accurate in making future PSA value predictions.

2. Clinical Trial Data

We use data from Bruchovsky et al. [9] in our analysis and model calibration. This clinical trial admitted patients who demonstrated a rising serum PSA level after they received radiotherapy and had no evidence of metastasis [9]. The treatment in each cycle consisted of administering cyproterone acetate for four weeks, followed by a combination of leuprolide acetate and cyproterone acetate, for an average of 36 weeks. If serum PSA is less than $4 \frac{\mu\text{g}}{\text{L}}$ by the end of this period, the androgen suppression therapy is stopped. If a patient's serum PSA stays above the threshold, the patient will be taken off of the study. After treatment is interrupted, PSA and androgen are monitored every four weeks. The therapy is restarted when patient's serum PSA increases to $\geq 10 \mu\text{g/L}$ [9]. The data set is available at [30]. Figure 1 shows a typical patient that undergoes IAS.

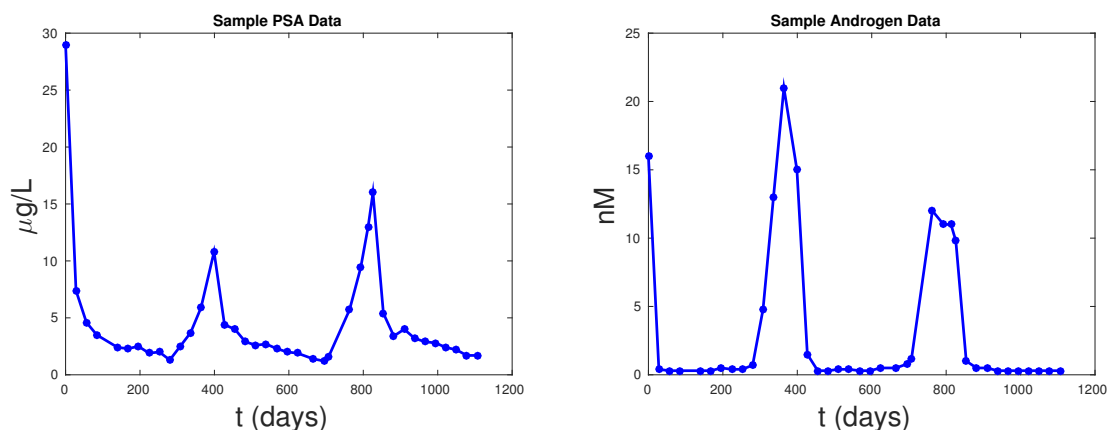


Figure 1. Sample data for prostate-specific antigen (PSA) and androgen data for a patient in a clinical trial.

3. Formulation of Mathematical Models

We develop two plausible mathematical models to study the temporal dynamics of prostate cancer progression to CRPR. In Model 1, we do not distinguish CS from CR cells. In this model, tumor cells' death rate is assumed to be a monotonically decreasing exponential function to implicitly account for the resistance development in cancer cells. Then, we propose a two cell population model where we separate CS from CR cells explicitly. To be more biologically relevant and consistent with the PKN model formulation, we assume in Model 2 that the development of cancer cell resistance to IAS is a decreasing function of androgen levels.

In both models, the cell growth rate is determined by the androgen *cell quota*. Specifically, as in the PKN model [13], we model the growth rate by a two parameter function of androgen cell quota,

$$G(Q) = \mu(1 - \frac{q}{Q}), \tag{1}$$

where Q is the androgen cell quota. Equation (1) is known as Droop equation or a Droop growth rate model [19]. It assumes that Q is the concentration of the most limiting resource or nutrient, and q is the minimum level of Q required to prevent cell death [27].

To be biologically relevant, for both models, we assume that the initial values for all variables are positive. This shall ensure that all components of their solutions are positive. Accordingly, we are only interested in studying the stabilities of nonnegative steady states and their biological and clinical implications.

3.1. Model 1: Single Population Model

In the following model, tumor cell volume is denoted by x (mm³), and we assume that the total volume is a combination of CS and CR cells. Intracellular androgen cell levels are denoted by Q (nM), and PSA levels by P ($\frac{\mu\text{g}}{\text{L}}$). Droop's equations govern the growth rate of cancer cells [27], where μ represents the maximum cell growth rate and q the minimum concentration of androgen to sustain the tumor. Similar to [28], we assume an androgen-dependent death rate, where R denotes the half saturation level. However, we also assume a time dependent maximum baseline death rate v , which decreases exponentially at rate d to reflect the cell castration-resistance development due to the decreasing death rate. We also include a density-independent death rate δ that constrains the total volume of cancer cells to be within realistic ranges [31]:

$$\frac{dx}{dt} = \underbrace{\mu(1 - \frac{q}{Q})x}_{\text{growth}} - \underbrace{(v\frac{R}{Q+R} + \delta x)x}_{\text{death}}, \tag{2}$$

$$\frac{dv}{dt} = -dv, \tag{3}$$

$$\frac{dQ}{dt} = \underbrace{\gamma}_{\text{production}} - \underbrace{(Q_m - Q)}_{\text{diffusion}} - \underbrace{\mu(Q - q)}_{\text{uptake}}, \tag{4}$$

$$\frac{dP}{dt} = \underbrace{bQ}_{\text{baseline}} + \underbrace{\sigma x Q}_{\text{tumor production}} - \underbrace{\epsilon P}_{\text{clearance}}, \tag{5}$$

$$\gamma = \gamma_1 u(t) + \gamma_2, \quad u(t) = \begin{cases} 1, & \text{on treatment,} \\ 0, & \text{off treatment.} \end{cases} \tag{6}$$

In this model, androgen is assumed to be the most limiting nutrient. We assume that the androgen concentration in cancer cells is approximately the same as the androgen concentration in serum [29]. Parameter γ_1 denotes the constant production of androgen by the testes, and γ_2 denotes the production of androgen by the adrenal gland and kidneys. As over 95% of androgen is produced in the testes, we have that $\gamma_1 \gg \gamma_2$. Parameter $u(t)$ is a switch between on and off treatment cycles. Luteinizing

hormone releasing hormone agonists only stop testes production of androgen during treatment. During treatment, γ_2 will be the only production of androgen. $Q_m > q$ denotes the maximum androgen level in serum. The androgen uptake by prostate cells is assumed to be proportional to the difference of the maximum possible and the current androgen levels in serum. Androgen in cells is depleted for growth at a rate of $\mu(Q - q)$. PSA is produced by both the regular cells in the prostate at the rate bQ and by the cancer cells at the rate σxQ . Notice that we have assumed that cell production of PSA is assumed to be dependent on levels of androgen. Finally, PSA is cleared from serum at rate ϵ .

3.2. Model 2: Two Population Model

Now, we present a two cell population model. In this model, we explicitly differentiate between CS and CR cells. x_1 (mm^3) and x_2 (mm^3) denote the CS and CR cell populations, respectively. The proliferation of each cancer cell population is denoted by

$$G_i(Q) = \mu\left(1 - \frac{q_i}{Q}\right), i = 1, 2,$$

for x_1 and x_2 respectively. Since CR cell populations proliferate at lower levels of androgen, we assume that $q_2 < q_1$. Death rates are denoted by:

$$D_i(Q) = d_i \frac{R_i}{Q + R_i}, i = 1, 2,$$

for their respective cell populations. We shall assume that $d_1 > d_2$, as CR cells are less susceptible to apoptosis by androgen deprivation than CS cells. Parameters $\delta_i, i = 1, 2$ denote the density dependent death rates, and we use these parameters to keep the maximum tumor volume in biological ranges.

Mutation between cell populations is assumed to take the form of a Hill equation of coefficient 1, given by:

$$\underbrace{\lambda(Q) = c \frac{K}{Q + K}}_{\text{CS to CR}}$$

The CS to CR rate, $\lambda(Q)$, is a decreasing function of the androgen levels. We assume that when cells are experiencing androgen depletion, they have higher selective pressure to develop resistance. Likewise, in an androgen rich environment, CS cells are more likely to stay sensitive. IAS started under this assumption, with the intention to delay resistance [10]. c is the maximum rate of mutation between cells and K is the cell concentration for achieving half of the maximum rate of mutation. In this model, d_i s are held constant and are not time dependent, as the mechanism of the development of resistance is due to mutations from x_1 to x_2 via $\lambda(Q)$ and not by a decreasing androgen dependent death rate.

The increase of intracellular androgen levels by diffusion from the serum level is modeled by $\gamma(Q_m - Q)$. For simplicity, and in contrast to the PKN model [13] and the model in Morken et al. [32], we assume the same PSA production rate σ for both cell populations:

$$\frac{dx_1}{dt} = \underbrace{\mu\left(1 - \frac{q_1}{Q}\right)x_1}_{\text{growth}} - \underbrace{(D_1(Q) + \delta_1 x_1)x_1}_{\text{death}} - \underbrace{\lambda(Q)x_1}_{\text{CS to CR}}, \tag{7}$$

$$\frac{dx_2}{dt} = \underbrace{\mu\left(1 - \frac{q_2}{Q}\right)x_2}_{\text{growth}} - \underbrace{(D_2(Q) + \delta_2 x_2)x_2}_{\text{death}} + \underbrace{\lambda(Q)x_1}_{\text{CS to CR}}, \tag{8}$$

$$\frac{dQ}{dt} = \underbrace{\gamma}_{\text{production}} \underbrace{(Q_m - Q)}_{\text{diffusion}} - \underbrace{\frac{\mu(Q - q_1)x_1 + \mu(Q - q_2)x_2}{x_1 + x_2}}_{\text{uptake}}, \tag{9}$$

$$\frac{dP}{dt} = \underbrace{bQ}_{\text{baseline}} + \underbrace{\sigma(Qx_1 + Qx_2)}_{\text{tumor production}} - \underbrace{\epsilon P}_{\text{clearance}}. \tag{10}$$

In a biologically realistic situation, one expects that $Q_m > \max\{q_1, q_2\}$.

3.3. Derivation of dQ/dt

Now, we provide a conservation law based derivation for the cell quota Q Equations (4) and (9). Specifically, we derive Equation (4) in detail and leave to the readers the straightforward task of its extension to (9). Our formulation comes from the conservation of androgen as it moves in and out of the tumor. Let Q_x be the total androgen inside tumor x (mm³). We assume that Q (nM) is uniformly distributed in x , and

$$Q_x = Q(t)x(t) \text{ nmol.}$$

The inflow of androgen to the tumor comes from the serum which can be approximated by

$$\gamma(Q_m - Q(t))x(t).$$

The outflow of androgen from the tumor is due to death, which is

$$\left(v \frac{R}{Q + R} + \delta x(t)\right)Q(t)x(t).$$

Then, the rate of change of androgen inside the tumor is:

$$(Q(t)x(t))' = \gamma(Q_m - Q(t))x(t) - \left(v \frac{R}{Q(t) + R} + \delta x(t)\right)Q(t)x(t).$$

However,

$$\begin{aligned} (Q(t)x(t))' &= Q'(t)x(t) + Q(t)x'(t) \\ &= Q'(t)x(t) + \mu(Q(t) - q)x(t) - \left(v \frac{R}{Q(t) + R} + \delta x(t)\right)Q(t)x(t), \end{aligned}$$

which implies that

$$Q'(t) = \gamma(Q_m - Q(t)) - \mu(Q(t) - q).$$

A similar approach can be applied to derive $Q'(t)$ for Model 2.

3.4. Portz, Kuang, and Nagy (PKN) Model

In this section, we briefly review the PKN model. For a more detailed explanation of this model, the reader is referred to [13]. The PKN model assumes constant death rates for cancer cells (d_1, d_2). CS and CR cells have androgen cell quota Q_1, Q_2 respectively. A denotes the serum androgen concentration, which is interpolated and used in the model:

$$\frac{dx_1}{dt} = \underbrace{\mu_m \left(1 - \frac{q_1}{Q_1}\right)x_1}_{\text{growth}} - \underbrace{d_1 x_1}_{\text{death}} - \underbrace{\lambda_1(Q_1)x_1}_{\text{CS to CR}} + \underbrace{\lambda_2(Q_2)x_2}_{\text{CR to CS}}, \tag{11}$$

$$\frac{dx_2}{dt} = \underbrace{\mu_m \left(1 - \frac{q_2}{Q_2}\right)x_2}_{\text{growth}} - \underbrace{d_2 x_2}_{\text{death}} - \underbrace{\lambda_2(Q_2)x_2}_{\text{CR to CS}} + \underbrace{\lambda_1(Q_1)x_1}_{\text{CS to CR}}, \tag{12}$$

$$\frac{dQ_1}{dt} = \underbrace{v_m \frac{q_m - Q_1}{q_m - q_1} \frac{A}{A + v_h}}_{\text{Androgen influx to CS cells}} - \underbrace{\mu(Q_1 - q_1)}_{\text{uptake}} - \underbrace{bQ_1}_{\text{degradation}}, \tag{13}$$

$$\frac{dQ_2}{dt} = \underbrace{v_m \frac{q_m - Q_2}{q_m - q_2} \frac{A}{A + v_h}}_{\text{Androgen influx to CR cells}} - \underbrace{\mu(Q_2 - q_2)}_{\text{uptake}} - \underbrace{bQ_2}_{\text{degradation}}, \tag{14}$$

$$\frac{dP}{dt} = \underbrace{\sigma_0(x_1 + x_2)}_{\text{baseline production}} + \underbrace{\sigma_1 x_1 \frac{Q_1^m}{Q_1^m + \rho_1^m}}_{\text{tumor production}} + \underbrace{\sigma_2 x_2 \frac{Q_2^m}{Q_2^m + \rho_2^m}}_{\text{tumor production}} - \underbrace{\delta P}_{\text{clearance}}. \tag{15}$$

4. Model Dynamics

Now, we study the mathematical properties and dynamics of our two models. For Model 1, we shall state the results without providing proofs as they are routine. The detailed mathematical analysis for Model 2 will be presented. Proposition 1 summarizes the mathematical dynamics of Model 1. Since P is decoupled from the system, we shall refer only to the dynamics of Equations (2)–(4). This proposition reveals that there is no cure for cancer. Since ADT is non-curative, this property is biologically reasonable.

Proposition 1. *Solutions of the system Equations (2)–(4) are positive and bounded. The system Equations (2)–(4) has a cancer free steady state $E_0 = (0, 0, \frac{\gamma Q_m + \mu q}{\mu + \gamma})$ that is unstable, and a steady state $E_1 = (\frac{\mu \gamma}{\delta} \frac{Q_m - q}{\gamma Q_m + \mu q}, 0, \frac{\gamma Q_m + \mu q}{\mu + \gamma})$ that is globally stable.*

Next, we do a thorough mathematical analysis of Model 2. First, we study boundedness and positivity of the system. Followed by the number and existence of steady states. Finally, we analyze the local stability of the steady states. Observe that P is also decoupled from Equations (2)–(4) and we do not include it in the analysis.

Proposition 2. *Assume $q_2 \leq q_1 < Q_m$ and $\delta_1 \geq \delta_2$. Then, solutions of Equations (7)–(9) with initial conditions $x_1(0) > 0, x_2(0) > 0$, and $q_2 \leq Q(0) \leq Q_m$ stay in the region $\{(x_1, x_2, Q) : x_1 \geq 0, x_2 \geq 0, x_1 + x_2 \leq \frac{G_2(Q_m) - D_m(q_2)}{\delta_2}, q_2 \leq Q \leq Q_m\}$, where $D_m = \min\{D_1(q_2), D_2(q_2)\}$.*

Proof. We note that in Equation (7), x_1 appears in every term ensuring its positivity. Since x_2 appears in the first two terms of (8) and x_1 appears in the last term, the positivity of x_2 is also guaranteed.

In addition, $q_2 \leq q_1 < Q_m$, and

$$Q' = \gamma(Q_m - Q) - \frac{\mu(Q - q_1)x_1 + \mu(Q - q_2)x_2}{x_1 + x_2}.$$

We see that $Q'(q_2) > 0$ and $Q'(Q_m) < 0$. It is thus easy to see that $q_2 \leq Q(t) \leq Q_m$ for $t > 0$ with initial conditions $q_2 \leq Q(0) \leq Q_m$.

For boundedness of x_1 and x_2 , we let $N = x_1 + x_2$. Since we have that $\delta_1 \geq \delta_2$, and the growth rate $G_i(Q), i = 1, 2$ are increasing functions of Q , we have

$$N' \leq (G_2(Q) - D_m)N - \delta_2 N^2, \tag{16}$$

$$\leq (G_2(Q_m) - D_m)N - \delta_2 N^2, \tag{17}$$

which implies that $\limsup_{t \rightarrow \infty} N(t) \leq \frac{G_2(Q_m) - D_m}{\delta_2}$. \square

Now, we study the steady states of Model 2. We seek to understand the conditions under which one population will overtake the other, and the circumstances under which they may coexist.

Proposition 3. *Assume $q_2 \leq q_1 < Q_m$ and $\delta_1 \geq \delta_2$. The system Equations (7)–(9) have a CR cell only steady state $E_1 = (0, \frac{G_2(Q^1) - D_2(Q^1)}{\delta_2}, Q^1)$, and a coexistence steady state $E_2 = (\frac{G_1(Q^*) - D_1(Q^*) - \lambda_1(Q^*)}{\delta_1}, x_2^*, Q^*)$, where $Q^1 = \frac{\gamma Q_m + \mu q_2}{\gamma + \mu}$ and $Q^* > Q^1$.*

Proof. Let $E = (x_1^*, x_2^*, Q^*)$ be a steady state of the system Equations (7)–(9). We have two mutually exclusive cases: $x_1^* = 0$ and $x_1^* > 0$.

If $x_1^* = 0$, then we have two possibilities: (i) $x_2^* = 0$ or (ii) $x_2^* > 0$. In the case of (i), we see that $E = E_0$. In the case of (ii), we see that $E = E_1$.

If $x_1^* > 0$, we see that $x_2^* > 0$ from the equation of dx_2/dt . In this case, $E = E_2$. In addition, we have the following:

$$\begin{aligned} 0 &= \gamma(Q_m - Q^*) - \frac{\mu(Q^* - q_1)x_1^* + \mu(Q^* - q_2)x_2^*}{x_1^* + x_2^*} \\ &\geq \gamma(Q_m - Q^*) - \mu(Q^* - q_2) \\ Q^* &\geq \frac{\gamma Q_m + \mu q_2}{\gamma + \mu} = Q^1. \end{aligned} \tag{18}$$

This proves the proposition. \square

Proposition 3 demonstrates that if the CS cell population survives, then the CR must also survive. Biologically, this makes sense, as the CR will always receive new mutated CR cells as ADT continues.

Next, we study the extinction of cancer cell populations and stability conditions for each of these steady states when feasible. Observe that we can not linearize at the steady state E_0 since the last term of dQ/dt is not differentiable at E_0 . This prevents us from carrying out a routine local stability analysis of E_0 .

Proposition 4 below simply confirms the intuition that if both cancer cell populations growth rates are too low, they will die out eventually. For ease of computations in the following propositions, we shall define $S_1(Q) = G_1(Q) - D_1(Q) - \lambda(Q)$ and $S_2(Q) = G_2(Q) - D_2(Q)$.

Proposition 4. Assume that $S_1(Q_m) < 0$, then CS population will die out. If, in addition, $S_2(Q_m) < 0$, then both cancer populations will die out.

Proof. Observe that both $S_1(Q)$ and $S_2(Q)$ are strictly increasing with respect to positive values of Q . Since,

$$\frac{x_1'(t)}{x_1(t)} = G_1(Q) - D_1(Q) - \lambda(Q) - \delta_2 x_1,$$

and $S_1(Q_m) < 0$, we know that $G_1(Q) - D_1(Q) - \lambda(Q) \leq S_1(Q_m) < 0$ for any Q . Let $m = -S_1(Q_m)$, and, since $x_1(t) > 0$, we have that

$$\begin{aligned} \frac{x_1'(t)}{x_1(t)} &\leq -m \\ x_1(t) &\leq ce^{-mt}. \end{aligned}$$

Therefore $\lim_{t \rightarrow \infty} x_1(t) = 0$. Applying a similar but slightly more delicate comparison argument to $x_2(t)$ with $\lim_{t \rightarrow \infty} x_1(t) = 0$ yields $\lim_{t \rightarrow \infty} x_2(t) = 0$. This completes the proof of this proposition. \square

The following proposition provides a simple set of conditions that yields the biologically realistic final outcome when sensitive cells are overtaken by resistant cells.

Proposition 5. The CR only steady state E_1 is locally asymptotically stable when $S_1(Q^1) < 0$ and $S_2(Q^1) > 0$.

Proof. The Jacobian matrix evaluated at E_1 is given by:

$$J(E_1) = \begin{pmatrix} S_1(Q^1) & 0 & 0 \\ \lambda(Q^1) & -S_2(Q^1) & \left(\frac{\mu q_2}{Q^2} + \frac{d_2}{(R_2+Q)^2}\right) \frac{G_2(Q^1) - D_2(Q^1)}{\delta_2} \\ \frac{\mu \delta_2 (q_1 - q_2)}{G_2(Q^1) - D_2(Q^1)} & 0 & -\gamma - \mu \end{pmatrix}.$$

The eigenvalues are the diagonal elements. We see that when $G_1(Q^1) - D_1(Q^1) - \lambda_1(Q^1) < 0$ and $G_2(Q^1) - D_2(Q^1) > 0$, all diagonal elements are negative. Hence, E_1 is locally asymptotically stable. \square

If both CS and CI cells can proliferate under treatment, then the coexistence equilibrium may be stable. Figure 2 displays the regions where this could happen. If CS cells have a high growth rate μ , they may survive under relatively low levels of androgen. Alternatively, if these cells have a very low death rate d_1 , they may persist as well.

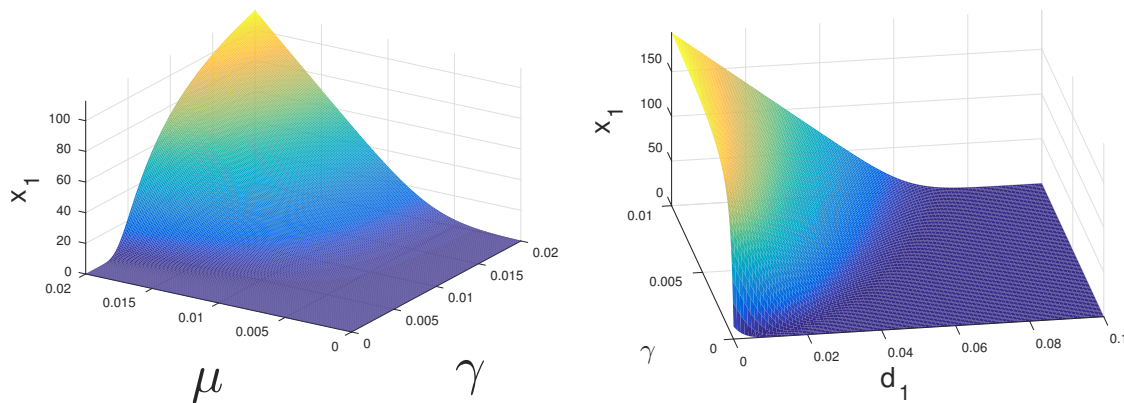


Figure 2. Bifurcation diagram displaying x_1 cell population vs. parameters μ and γ (left) and γ and d_1 (right). This figure depicts the regions in which x_1 can go extinct. This happens when androgen levels γ are very low, or cancer cells' proliferation rate μ is very low, or cancer cells' death rate d_1 is very high.

5. Parameter Estimation

In order to perform realistic model simulations, we need to obtain reasonable parameter values and their ranges. We start by estimating the realistic ranges for each of them. Parameters μ , d_1, d_2 are taken from [33], where they assess the growth and death rates of prostate cells under different concentrations of androgen. In [12], it was shown that, under continuous treatment, the fastest resistance rate is $c \approx 0.0001$. The approximate levels at which sensitive and resistant cells proliferate was studied in [34], from which we approximated q, q_1 , and q_2 .

In patients with no prostate cancer, PSA levels are usually less than $5 \frac{\mu\text{g}}{\text{L}}$, accounting for benign tumor hyperplasia [8]. This implies that when tumor volume is near zero, the steady state of PSA given by: $\frac{bQ}{\epsilon}$ shall be approximately $5 \frac{\mu\text{g}}{\text{L}}$. Prostate tumor volumes are normally bounded by 80 mm in length and, on average, they are about 13.4 mm [31]. Since all of our patients have advanced prostate cancer, we assumed a maximum length of 40 mm, and we compute the corresponding tumor volume assuming that tumors are spherical. Under complete androgen independence, tumor volume should not exceed $700 \text{ (mm}^3\text{)}$. Thus, $\frac{\mu}{\delta} \approx \frac{\mu}{\delta_2} + \frac{\mu}{\delta_2} \approx 700 \text{ (mm}^3\text{)}$. Parameter Q_m is patient specific and is taken from the maximum androgen serum concentration of each patient during the first 1.5 cycles of treatment. Parameter γ_1 is held constant among every patient and γ_2 has a range of $0-0.01 \frac{\text{nmol}}{\text{Lday}}$. The half-saturation variables $K, R, R1$, and $R2$ are estimated from [28]. Table 1 shows definitions, ranges, units, and sources for each of the parameters in our models.

Table 1. Parameter definitions, units, and ranges.

Parameters	Definition	Range	Units	Source
μ	Maximum proliferation rate	0.001–0.09	day ⁻¹	[33]
q	Minimum cell quota	0.1–0.5	nM	[34]
q_1	Minimum CS cell quota	0.1–0.5	nM	[34]
q_2	Minimum CR cell quota	0.1–0.3	nM	[34]
b	Prostate baseline PSA	0.1–2.5	10 ⁻³ µg/L/nM/day	[9]
σ	Tumor PSA production rate	0.001–0.9	µg/L/nM/mm ³ /day	[28]
ϵ	PSA clearance rate	0.001–0.01	day ⁻¹	[28]
d	Maximum cell death rate	0.0001–0.09	day ⁻¹	[33]
d_1	Maximum CS cell death rate	0.001–0.09	day ⁻¹	[33]
d_2	Maximum CR cell death rate	0.0001–0.001	day ⁻¹	[33]
δ_1	Density death rate	0.1–9 × 10 ⁻⁵	1/day/mm ³	[31]
δ_2	Density death rate	0.01–4.5 × 10 ⁻⁴	1/day/mm ³	[31]
R	Cell death rate half-saturation level	0–3	nM	[28]
R_1	CS cell death rate half-saturation level	0–3	nM	[28]
R_2	CR cell death rate half-saturation level	0–3	nM	[28]
c_1	Maximum CS to CR rate	10 ⁻⁵ –10 ⁻⁴	day ⁻¹	[12]
K	CS to CR half-saturation level	0–1	nM	[28]
γ_1	Testes androgen production	20	day ⁻¹	ad hoc
γ_2	Secondary androgen production	0.001–0.01	day ⁻¹	ad hoc
Q_m	Maximum androgen	15–30	nM	[9]
ν	death rate decay rate	0.01	unitless	ad hoc

5.1. Sensitivity Analysis

Sensitivity analysis can be used to show which parameters play a bigger role in a model. The normalized sensitivity, S_p , for parameter p and state variable x is given by:

$$S_p = \frac{\partial x}{\partial p} \frac{p}{x}.$$

Figure 3 shows the sensitivities of every parameter and state variable for Model 1. We observe that, with the exception of d , no parameter has a much larger sensitivity than the rest. d is the only parameter that can dramatically affect cancer cell death rate, and we see a spike in the sensitivity figures. Cancer cell growth rate μ has the greatest effect on androgen and cancer cells, whereas σ and ϵ play the greatest roles in PSA production. Figure 4 shows the sensitivity of each parameter in Model 2. We see similarities with Model 1 in that μ affects the production androgen and CR cells the most. In addition, PSA production is affected by the same parameters as in Model 1. Notice that CS cells are affected by d_1 the most since they are the most susceptible to changes in the androgen concentration.

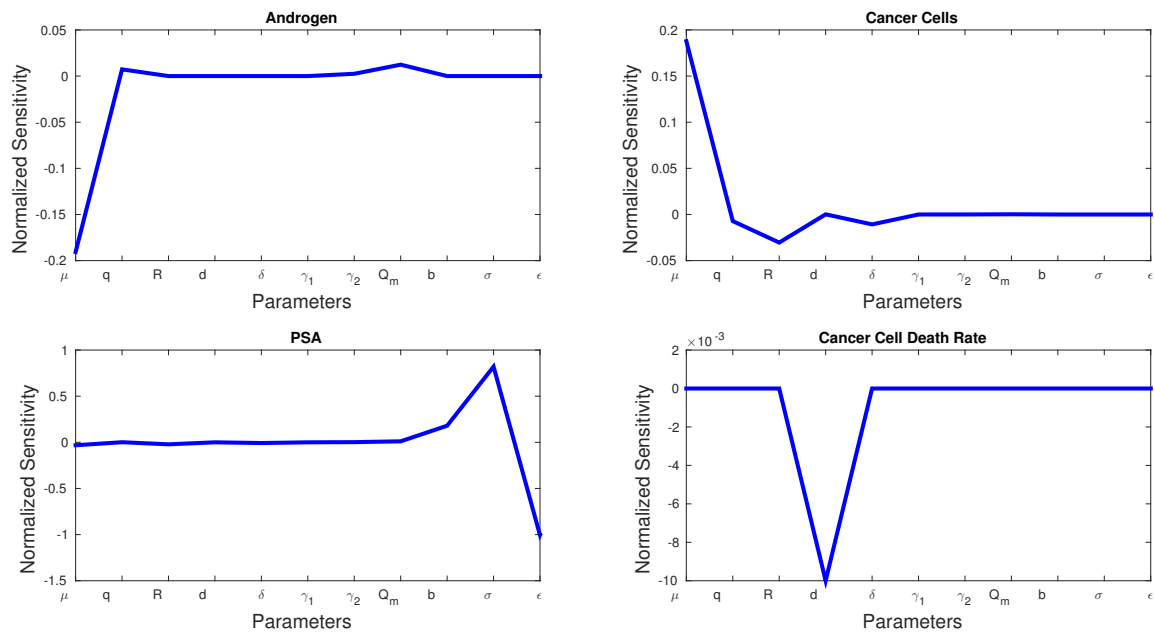


Figure 3. Normalized sensitivities of Model 1.

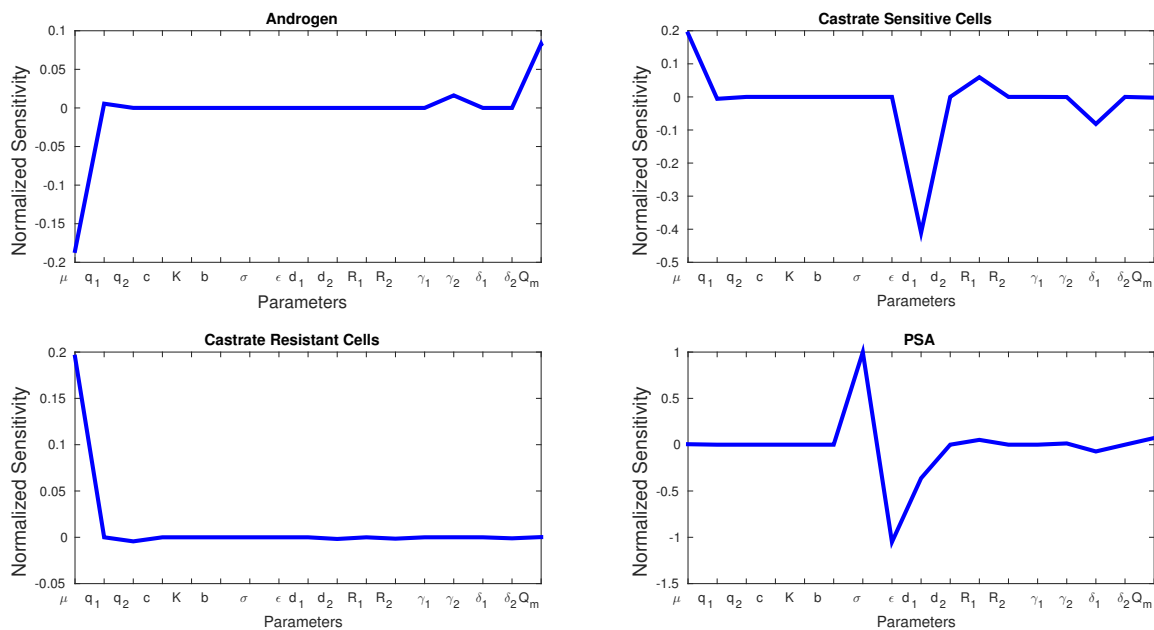


Figure 4. Normalized sensitivities of Model 2.

6. Comparison of Models

We use data from the Vancouver Prostate Center (Vancouver, BC, Canada) to validate and compare the accuracy of each model. From the 109 patients registered, 103 were eligible for interruption of treatment, with a PSA response rate of 95% [9]. Using the criteria of having at least 20 data points for both androgen and PSA in the initial 1.5 cycles, we select 62 from those 109 patients. The individual PSA and androgen mean square error (MSE) are provided in Table 2 from these 62 selected patients. Notice that the PKN model did not include an androgen equation, and thus we cannot compare the fittings of androgen with the PKN model.

For the PKN model, we interpolated androgen serum data using a cubic spline interpolation between every androgen data point. This created a function in terms of time that was utilized as A in

(13) and (14). We implemented the method used by Portz et al. [13] for generating future androgen levels by generating a rectangular function based on the average off and on-treatment serum androgen values. Parameter ranges were taken from PKN [13] and Everett et al. [28], and the reader is referred to these papers for more details on forecasting serum PSA levels and parameter values of the PKN model. For every patient selected, we fitted 1.5 cycles of treatment and performed parameter estimation. Then, to measure the forecasting ability of every model, we ran the models for one more cycle of data using the parameters estimated from the initial 1.5 cycles.

Table 2. Comparison of Mean Squared Error (MSE) for Androgen and prostate-specific antigen (PSA) for the first 1.5 cycles.

Model	PSA			Androgen		
	Min	Mean	Max	Min	Mean	Max
PKN Model	0.5119	9.4463	93.1587	N/A	N/A	N/A
Model 1	0.9735	8.6763	71.8471	5.0351	100.1071	710.2604
Model 2	0.2461	10.3993	137.4345	5.1283	101.4763	710.4412

To compare models, we conduct simulations with MATLAB’s (MATLAB 9.1, The MathWorks, Inc., Natick, MA, USA) built in function `fmincon`, which uses the Interior Point Algorithm, to find the optimum parameters for each patient. The algorithm searches for a minimum value in a range of pre-specified parameter ranges, which we estimated from various literature sources. We use this algorithm to minimize the MSE for PSA and androgen data. The MSE is calculated with the following equations:

$$P_{error} = \frac{\sum_{i=1}^N (P_i - \hat{P}_i)^2}{N},$$

$$Q_{error} = \frac{\sum_{i=1}^N (Q_i - \hat{Q}_i)^2}{N},$$

where N represents the total number of data points, P_i represents the PSA data value, and \hat{P}_i the value from the model. Likewise, Q_i represents the androgen data value, and \hat{Q}_i the value from the model. We then use an equally weighted combination of both errors

$$error = P_{error} + Q_{error},$$

as our objective function, which is then minimized with `fmincon`.

Figure 5 shows PSA fitting and forecasting simulations for patients 1, 15, 17, and 63. We selected these patients to display the typical behavior shown in all 62 patients. Patient 1 shows that Models 1, 2, and PKN fit data with about the same accuracy. However, PKN overshoots in forecasting and Model 2 outperforms Model 1 in forecasting. Patient 17 shows that PKN underestimates future PSA levels, but Models 1 and 2 both perform well. Patients 15 and 63 provide the cases where PKN does a better forecast while Models 1 and 2 still do better. The rest of the patients can be classified similarly.

Table 2 documents the error of fitting 1.5 cycles of treatment and Table 3 displays the errors in forecasting one more cycle of treatment. On average, PKN and Model 1 perform prediction at the same level of accuracy. However, Model 2 performs prediction on average about three times better than the PKN model and Model 1.

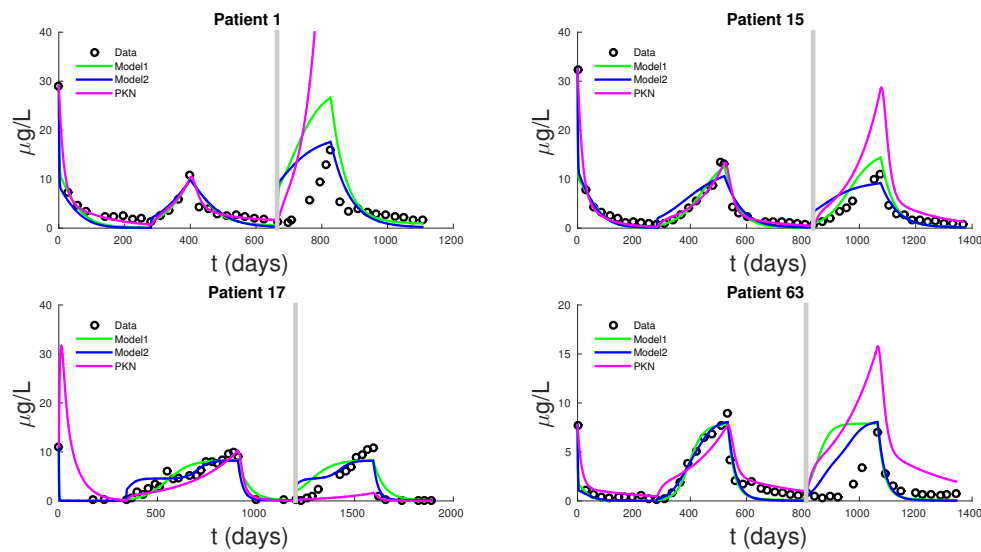


Figure 5. Simulations of fittings for every model for 1.5 cycles of treatment (left of gray line), and one cycle of forecast (right of gray line). For these four patients, we can see that models fit data at comparable accuracy but Model 2 perform much better in PSA forecasting.

Table 3. Comparison of forecast Mean Square Error for PSA.

Model	Min	Mean	Max
PKN Model	12.234	162.5494	1868.6394
Model 1	11.3935	141.9280	1663.0218
Model 2	2.2727	56.3478	278.4050

7. Conclusions

The main goal of this research is to produce a basic model capable of describing prostate cancer cell growth subject to IAS. Such a model may be amendable to detailed and systematical mathematical and computational study aimed at revealing the near term and intermediate term growth dynamics, including cancer cells treatment resistance development. Ultimately, such models may be helpful in establishing user-friendly treatment tools for both patients and physicians. To this end, we presented two models that can accurately fit clinical PSA and androgen data simultaneously. Existing models can only fit the PSA data. While these models are simplifications of PKN, they are just as accurate in data fitting and even better at forecasting future PSA levels. Model 1 had the lowest mean MSE for data fitting of all the models, followed by PKN and Model 2—not surprisingly, due to its more biologically realistic model assumptions, Model 2 had the lowest forecast MSE, with PKN doing the worst. The unreliability of PKN’s forecasts stems from its dependence on androgen data and hence lacks the ability to predict androgen dynamics. Androgen cell quota values, which are not directly measurable from data, represent a significant source of uncertainty for the PKN model. Figure 6, shows how the new models can fit clinical androgen data and reduce uncertainty. For Models 1 and 2, Q is directly computable from clinical data.

Predicting the timing of resistance is a highly desirable objective of this modeling work. Mathematical models alone can not make practical predictions. However, we can use these models and apply statistical methods to produce reliable forecasts with confidence intervals [35,36]. In Pell et al. [35] and Chowell et al. [36], the authors have used these methods successfully in an epidemiological setting to make predictions. In a future paper, the authors plan to use the models presented in this paper to produce predictions using such statistical methods. Therefore, the main biological contribution

of this work is the development of a clear and basic androgen cell-quota based model to aid our understanding of the resistance development dynamics of prostate cancer cells.

The dynamics of Model 1 is characterized by globally stable steady states. The mathematical analysis of Model 2 is only partially tractable. In fact, the stability and global stability of the cancer cell coexistence steady state remain unsettled. However, with our bifurcation analysis, we observe that under ADT or IAS, x_2 cells may drive x_1 cells to extinction. In Figure 2, we see that with lower and realistic levels of androgen production when the patient is under ADT, x_1 cells will eventually become extinct even at a higher level of proliferation compared to x_2 cells. Thus, we concluded that, under continuous treatment, almost all patients will eventually become androgen resistant. However, it is still not clear if IAS delays the speed at which this occurs. With the models presented in this work, we have moved closer to the ultimate goal of modeling the androgen resistance of prostate cancer.

Our work is limited by the small number of patients considered. We selected 62 patients that had at least 20 data points in the first 1.5 cycles of treatment. Using a larger time interval and more patients to calibrate models might reveal more subtle differences in the models' ability to fit data. Additionally, tumor volume data will allow us to validate the model more naturally. Figures 7 and 8 show the cancer populations for Models 1 and 2 in resistant and non-resistant patients. Tumor volume data will allow us to verify the results in these figures even if only a few data points are available.

In addition, identifiability analysis to determine if our parameter values can be represented uniquely by clinical data is essential if these models are to be used in a clinical setting to reliably and accurately predict PSA dynamics for individual patients. Allowing parameters to vary as treatment progresses and studying the changes in key parameter values such as proliferation and death rates as functions of time might be useful to describe and predict resistance mechanisms as suggested in the work of Morken et al. [32].

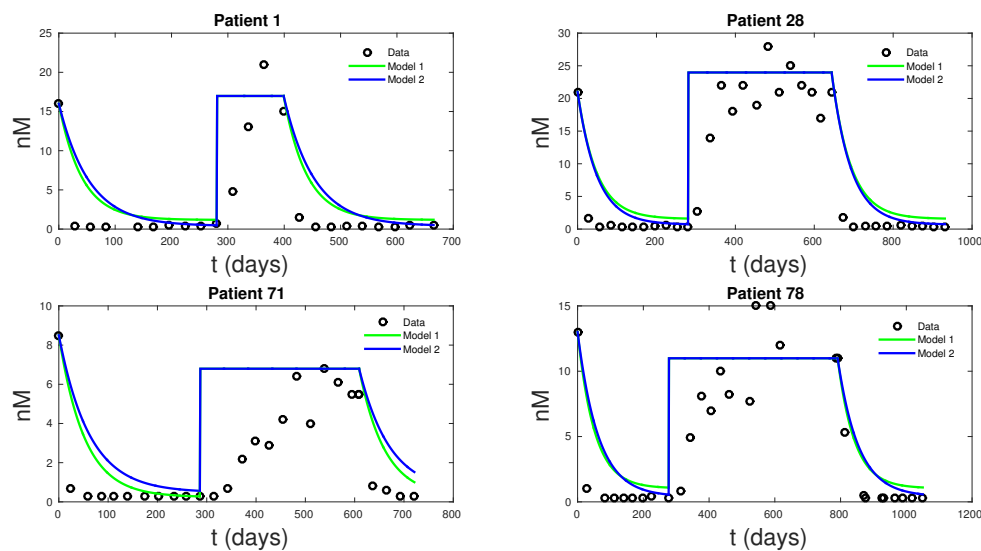


Figure 6. Simulations of fittings of androgen levels for Models 1 and 2. These two models have comparable goodness in fitting androgen data as their derivations are very similar.

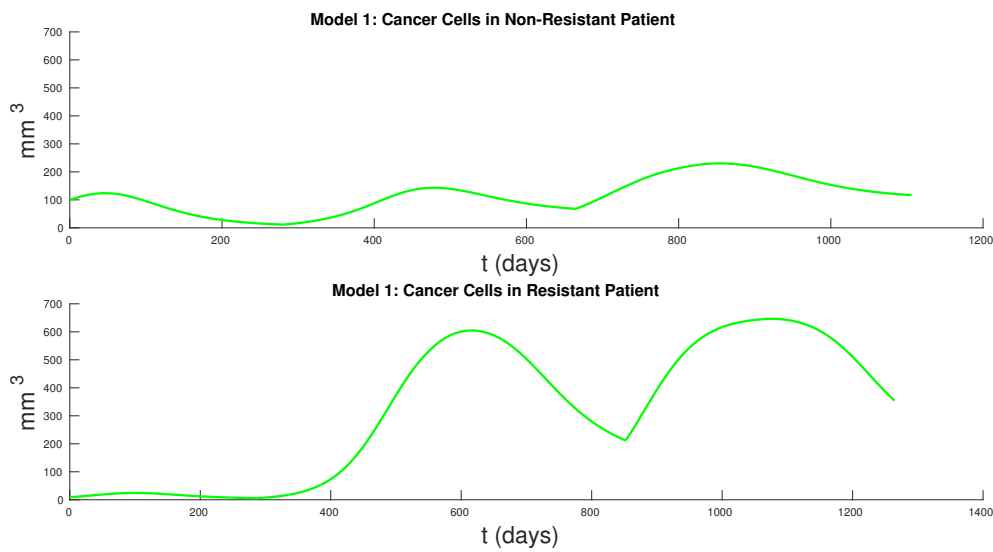


Figure 7. Cancer cells in resistant and non-resistant patient for Model 1. For the non-resistant patient we see a slight increase in volume over the course of several cycles. In the resistant patient we see that cancer volume has grown substantially.

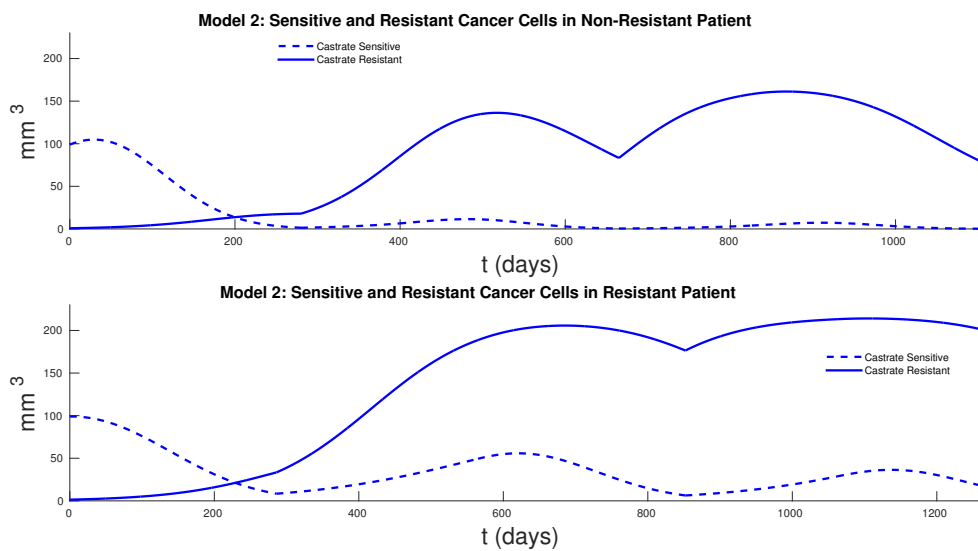


Figure 8. Cancer cells in resistant and non-resistant patients for Model 2. For the non-resistant patient, we see an increase in the volume of CR cells, but the original volume is about the same. In the resistant patient, we see that cancer volume has grown to double the volume compared to the non resistant patient.

Acknowledgments: The authors are partially supported by a US NSF grant DMS-1518529 and are profoundly grateful to Nicholas Bruchovsky for the clinical data set and his encouragement. In addition, the authors would like to thank Tin Phan and the reviewers for many helpful comments that improved the presentation of this manuscript.

Author Contributions: J.B. and Y.K. conceived and designed the models; J.B. created the code and ran simulations; J.B. and Y.K. wrote the paper.

Conflicts of Interest: The authors declare no conflict of interest.

References

1. Heinlein, C.; Chang, C. Androgen receptor in prostate cancer. *Endocr. Rev.* **2004**, *25*, 276–308.
2. Shafi, A.; Yen, A.; Weigel, N. Androgen receptors in hormone-dependent and castration-resistant prostate cancer. *Pharmacol. Ther.* **2013**, *140*, 223–238.
3. Tsao, C.K.; Small, A.; Galsky, M.; Oh, W. Overcoming castration resistance in prostate cancer. *Curr. Opin. Urol.* **2012**, *22*, 167–174.
4. Bruchovsky, N.; Klotz, L.; Crook, J.; Phillips, N.; Abersbach, J.; Goldenberg, S. Quality of life, morbidity, and mortality results of a prospective phase II study of intermittent androgen suppression for men with evidence of prostate-specific antigen relapse after radiation therapy for locally advanced prostate cancer. *Clin. Genitourin. Cancer* **2008**, *6*, 46–52.
5. Feldman, B.; Feldman, D. The development of androgen-independent prostate cancer. *Nat. Rev. Cancer* **2001**, *1*, 34–45.
6. Hussain, M.; Tangen, C.; Berry, D.; Higano, C.; Crawford, E.; Liu, G.; Wilding, G.; Prescott, S.; Sundaram, S.K.; Small, E.J.; et al. Intermittent versus continuous androgen deprivation in prostate cancer. *N. Engl. J. Med.* **2013**, *368*, 1314–1325.
7. Karantanos, T.; Evans, C.P.; Tombal, B.; Thompson, T.C.; Montironi, R.; Isaacs, W.B. Understanding the mechanisms of androgen deprivation resistance in prostate cancer at the molecular level. *Eur. Urol.* **2015**, *67*, 470–479.
8. Klotz, L.; Toren, P. Androgen deprivation therapy in advanced prostate cancer: Is intermittent therapy the new standard of care? *Curr. Oncol.* **2012**, *19*, S13–S21.
9. Bruchovsky, N.; Klotz, L.; Crook, J.; Malone, S.; Ludgate, C.; Morris, W.J.; Gleave, M.E.; Goldenberg, S.L. Final results of the Canadian prospective phase II trial of intermittent androgen suppression for men in biochemical recurrence after radiotherapy for locally advanced prostate cancer. *Cancer* **2006**, *107*, 389–395.
10. Gleave, M. Prime time for intermittent androgen suppression. *Eur. Urol.* **2014**, *66*, 240–242.
11. Jackson, T. A Mathematical Investigation of the Multiple Pathways to Recurrent Prostate Cancer: Comparison with Experimental Data. *Neoplasia* **2004**, *6*, 697–704.
12. Ideta, A.; Tanaka, G.; Takeuchi, T.; Aihara, K. A mathematical model of intermittent androgen suppression for prostate cancer. *J. Nonlinear Sci.* **2008**, *18*, 593–614.
13. Portz, T.; Kuang, Y.; Nagy, J. A clinical data validated mathematical model of prostate cancer growth under intermittent androgen suppression therapy. *AIP Adv.* **2012**, *2*, 1–14.
14. Hirata, Y.; Bruchovsky, N.; Aihara, K. Development of a mathematical model that predicts the outcome of hormone therapy for prostate cancer. *J. Theor. Biol.* **2010**, *264*, 517–527.
15. Swanson, K.; True, L.; Lin, D.; Buhler, K.; Vessella, R.; Murray, J. A quantitative model for the dynamics of serum prostate-specific antigen as a marker for cancerous growth: An explanation for a medical anomaly. *Am. J. Pathol.* **2001**, *158*, 2195–2199.
16. Jain, H.; Clinton, S.; Bhinder, A.; Friedman, A. Mathematical modeling of prostate cancer progression in response to androgen ablation therapy. *Proc. Natl. Acad. Sci. USA* **2011**, *108*, 19701–19706.
17. Jain, H.; Friedman, A. Modeling prostate cancer response to continuous versus intermittent androgen ablation therapy. *Discret. Contin. Dyn. Syst. B* **2013**, *18*, 945–967.
18. Jain, H.; Friedman, A. A partial differential equation model of metastasized prostatic cancer. *Math. Biosci. Eng.* **2013**, *10*, 591–608.
19. Kuang, Y.; Nagy, J.; Eikenberry, S. *Introduction to Mathematical Oncology*; CRC Press: Boca Raton, FL, USA, 2016.
20. Guo, Q.; Lu, Z.; Hirata, Y.; Aihara, K. Parameter estimation and optimal scheduling algorithm for a mathematical model of intermittent androgen suppression therapy for prostate cancer. *Chaos* **2013**, *23*, 43125.
21. Tao, Y.; Guo, Q.; Aihara, K. A partial differential equation model and its reduction to an ordinary differential equation model for prostate tumor growth under intermittent hormone therapy. *J. Math. Biol.* **2014**, *69*, 817–838.
22. Suzuki, Y.; Sakai, D.; Nomura, T.; Hirata, Y.; Aihara, K. A new protocol for intermittent androgen suppression therapy of prostate cancer with unstable saddle-point dynamics. *J. Theor. Biol.* **2014**, *350*, 1–16.

23. Hirata, Y.; Akakura, K.; Higano, C.; Bruchovsky, N.; Aihara, K. Quantitative mathematical modeling of PSA dynamics of prostate cancer patients treated with intermittent androgen suppression. *J. Mol. Cell Biol.* **2012**, *4*, 127–132.
24. Hirata, Y.; Tanaka, G.; Bruchovsky, N.; Aihara, K. Mathematically modelling and controlling prostate cancer under intermittent hormone therapy. *Asian J. Androl.* **2012**, *14*, 270–277.
25. Hirata, Y.; Azuma, S.; Aihara, K. Model predictive control for optimally scheduling intermittent androgen suppression of prostate cancer. *Methods* **2014**, *67*, 278–281.
26. Jackson, T. A mathematical model of prostate tumor growth and androgen-independent relapse. *Discret. Contin. Dyn. Syst. B* **2004**, *4*, 187–202.
27. Droop, M. Some thoughts on nutrient limitation in algae1. *J. Phycol.* **1973**, *9*, 264–272.
28. Everett, R.; Packer, A.; Kuang, Y. Can Mathematical Models Predict the Outcomes of Prostate Cancer Patients Undergoing Intermittent Androgen Deprivation Therapy? *Biophys. Rev. Lett.* **2014**, *9*, 173–191.
29. Roy, A.; Chatterjee, B. Androgen action. *Crit. Rev. Eukaryot. Gene Expr.* **1995**, *5*, 157–176.
30. Bruchovsky, N. Clinical Research. 2006. Available online: <http://www.nicholasbruchovsky.com/clinicalResearch.html> (accessed on 11 November 2016).
31. Vollmer, R. Tumor Length in Prostate Cancer. *Am. J. Clin. Pathol.* **2008**, *130*, 77–82.
32. Morken, J.; Packer, A.; Everett, R.; Nagy, J.; Kuang, Y. Mechanisms of resistance to intermittent androgen deprivation in patients with prostate cancer identified by a novel computational method. *Cancer Res.* **2014**, *74*, 3673–3683.
33. Berges, R.R.; Vukanovic, J.; Epstein, J.I.; CarMichel, M.; Cisek, L.; Johnson, D.E.; Veltri, R.W.; Walsh, P.C.; Isaacs, J.T. Implication of cell kinetic changes during the progression of human prostatic cancer. *Clin. Cancer Res.* **1995**, *1*, 473–480.
34. Nishiyama, T. Serum testosterone levels after medical or surgical androgen deprivation: A comprehensive review of the literature. *Urol. Oncol.* **2013**, *32*, 38.e17–38.e28.
35. Pell, B.; Baez, J.; Phan, T.; Gao, D.; C, G.; Kuang, Y. *Patch Models of EVD Transmission Dynamics*; Springer: Cham, Switzerland, 2016.
36. Chowell, G.; Simonsen, L.; Kuang, Y.; Sciences, S. Is West Africa Approaching a Catastrophic Phase or is the 2014 Ebola Epidemic Slowing Down? Different Models Yield Different Answers for Liberia. *PLOS Curr. Outbreaks* **2014**, doi:10.1371/currents.outbreaks.b4690859d91684da963dc40e00f3da81.



© 2016 by the authors; licensee MDPI, Basel, Switzerland. This article is an open access article distributed under the terms and conditions of the Creative Commons Attribution (CC-BY) license (<http://creativecommons.org/licenses/by/4.0/>).